ARTICLES

The origin of spontaneous activity in the developing auditory system

Nicolas X. Tritsch[1], Eunyoung Yi[2], Jonathan E. Gale[3], Elisabeth Glowatzki[1,2] & Dwight E. Bergles[1,2]

Spontaneous activity in the developing auditory system is required for neuronal survival as well as the refinement and maintenance of tonotopic maps in the brain. However, the mechanisms responsible for initiating auditory nerve firing in the absence of sound have not been determined. Here we show that supporting cells in the developing rat cochlea spontaneously release ATP, which causes nearby inner hair cells to depolarize and release glutamate, triggering discrete bursts of action potentials in primary auditory neurons. This endogenous, ATP-mediated signalling synchronizes the output of neighbouring inner hair cells, which may help refine tonotopic maps in the brain. Spontaneous ATP-dependent signalling rapidly subsides after the onset of hearing, thereby preventing this experience-independent activity from interfering with accurate encoding of sound. These data indicate that supporting cells in the organ of Corti initiate electrical activity in auditory nerves before hearing, pointing to an essential role for peripheral, non-sensory cells in the development of central auditory pathways.

Auditory perception depends on the precise conversion of sound-induced vibrations of the basilar membrane into graded release of transmitter from inner hair cells (IHCs), which provide the main excitatory input to auditory nerve fibres. The immaturity of the middle and inner ear of newborn rats prevents the detection of airborne sounds before the 'onset of hearing'—the age range over which neonates first display sound-evoked neural responses (postnatal day (P)11–13)[1,2]. Nevertheless, IHCs can release glutamate in a Ca^{2+}-dependent manner[3] and auditory nerves fire discrete bursts of action potentials before the onset of hearing[4–7], suggesting that spiral ganglion neurons (SGNs) are subjected to periodic excitation. This spontaneous activity is abolished after cochlea removal or application of the sodium channel blocker tetrodotoxin (TTX) to the oval window[8], indicating that the trigger for this activity resides within the cochlea. However, the mechanisms responsible for initiating auditory nerve firing in the absence of sound have not been determined.

Spontaneous ATP release in the developing cochlea

The developing cochlea of mammals contains a transient structure of unknown function termed Kölliker's organ (or greater epithelial ridge), consisting of a wide expanse of columnar-shaped supporting cells[9–11] (Fig. 1a). In cochlear turns acutely isolated from rats before the onset of hearing, we observed spontaneous inward currents in whole-cell voltage-clamp recordings from these 'inner' supporting cells. These events occurred at a frequency of 0.20 ± 0.01 Hz, varied widely in amplitude (mean = -254 ± 20 pA, coefficient of variance = 1.48 ± 0.03) and exhibited remarkably slow kinetics (mean rise time, $t_{rise} = 1{,}546 \pm 51$ ms, $n = 23$; Fig. 1b). Despite their low input resistance (7.4 ± 0.4 MΩ, $n = 16$), inner supporting cells were depolarized by as much as 37 mV by these spontaneous inward currents (Fig. 1c). When a field electrode was inserted within Kölliker's organ, spontaneous extracellular potentials up to 5 mV in amplitude (mean = 0.21 ± 0.01 mV, $n = 66$) were observed; these responses exhibited slow kinetics ($t_{rise} = 1{,}098 \pm 47$ ms) and occurred with a frequency similar to that of spontaneous inward currents (0.19 ± 0.01 Hz; Fig. 1d). In simultaneous recordings, 85% of spontaneous extracellular potentials were coincident with spontaneous inward currents in nearby supporting cells ($n = 447$ field potentials in seven pairs; Supplementary Fig. 1), suggesting that extracellular potentials result from the spontaneous currents. These results indicate that there is widespread intrinsic activity in the developing cochlea, which can be detected as inward currents in supporting cells and local field potentials within Kölliker's organ.

To determine the mechanisms responsible for this spontaneous activity, we applied pharmacological inhibitors of receptors known to be expressed in the developing cochlea[12]. Field potentials were not altered by the $\alpha_9\alpha_{10}$ acetylcholine receptor antagonist strychnine ($n = 5$, $P > 0.7$), the muscarinic receptor antagonist atropine ($n = 4$, $P > 0.7$), or the nicotinic receptor antagonist D-tubocurarine (D-TC, $n = 4$, $P > 0.4$), indicating that this spontaneous activity was not initiated by cholinergic efferents[13]. These events also did not require Ca^{2+}-dependent release of glutamate from IHCs or neuronal firing, as they were not affected by cadmium ($n = 4$, $P > 0.1$) or nifedipine ($n = 4$, $P > 0.9$), which inhibit IHC Ca^{2+} currents[14], by the glutamate receptor antagonists 2,3-dihydroxy-6-nitro-7-sulphamoyl-benzo(f)quinoxaline (NBQX, $n = 4$, $P > 0.8$) and *R*,*S*-3-(2-carboxypiperazin-4-yl)propyl-1-phosphonic acid (*R*,*S*-CPP, $n = 3$, $P > 0.5$), or by TTX ($n = 3$, $P > 0.6$) (Fig. 1e and Supplementary Fig. 2). However, spontaneous extracellular potentials were significantly inhibited by the P2 purinergic receptor antagonists pyridoxal-phosphate-6-azophenyl-2', 4'-disulphonate (PPADS, $n = 5$, $P < 0.0001$) and suramin ($n = 6$, $P < 0.0005$), but not the adenosine receptor antagonist 1,3-dipropyl-8-cyclopentylxanthine (DPCPX, $n = 4$, $P > 0.4$), suggesting that this spontaneous cochlear activity was initiated by extracellular ATP (Fig. 1d, e and Supplementary Fig. 2). Consistent with this hypothesis, both the frequency and amplitude of spontaneous extracellular potentials were significantly decreased by the ATP-hydrolysing enzyme apyrase ($n = 5$, $P < 0.005$). Moreover, in whole-cell recordings from inner supporting cells, application of ATP, but not adenosine, induced large inward currents (4.1 ± 0.8 nA, $n = 7$; Supplementary Fig. 3), indicating that ATP is sufficient to elicit this activity.

[1]The Solomon H. Snyder Department of Neuroscience, [2]The Center for Hearing and Balance, Department of Otolaryngology—Head and Neck Surgery, Johns Hopkins School of Medicine, Baltimore, Maryland 21205, USA. [3]UCL Ear Institute and Department of Physiology, University College London, London WC1X 8EE, UK.

Extracellular ATP exerts modulatory effects by binding to ionotropic (P2X) and metabotropic (P2Y) purinergic receptors in target tissues[15], and members of both receptor classes are expressed in the developing organ of Corti[16]. Indeed, ATP-evoked currents in inner supporting cells exhibited prominent inward rectification and reversed near 0 mV ($n = 5$; Supplementary Fig. 3), properties consistent with recombinant P2X receptors[17]. Large inward currents were also elicited in supporting cells by the P2Y receptor agonist UTP ($n = 6$; Supplementary Fig. 3), suggesting that both P2X and P2Y receptors contribute to the ATP-dependent activity observed in Kölliker's organ.

Studies of epithelial cells in the periphery and glia cells in the central nervous system indicate that ATP can be released through large transmembrane pores such as $P2X_7$ receptors or unpaired connexons, termed hemichannels[18]. Cochlear supporting cells are extensively coupled through gap junctions, and connexin 26, which is highly expressed by these cells[19], has been shown to allow the passage of large anions, such as ATP[20]. ATP-dependent spontaneous activity in Kölliker's organ was blocked by the gap junction inhibitors octanol ($n = 6$, $P < 0.0001$) and carbenoxolone (CBX, $n = 4$, $P < 0.0001$). In addition, the frequency of spontaneous extracellular potentials was markedly increased by exposure to Ca^{2+}-free solution, a manipulation that opens hemichannels[18], and this increase in activity was inhibited by PPADS ($n = 4$, $P < 0.018$; Fig. 1e). Conversely, spontaneous activity was not affected by the $P2X_7$ receptor antagonist brilliant blue G ($n = 5$, $P > 0.3$; Supplementary Fig. 2). These results suggest that gap junctions, and perhaps unpaired connexon hemichannels, are required for ATP release in the developing cochlea.

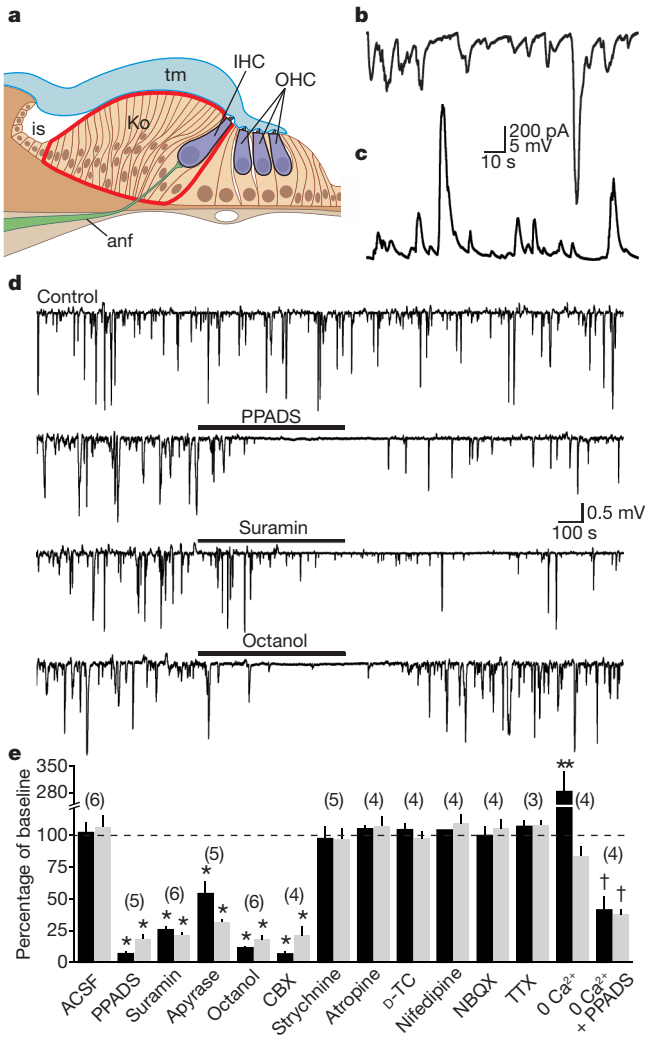

Figure 1 | Spontaneous purinergic signalling in the developing cochlea. **a**, Diagram of a P7 rat organ of Corti in cross-section. anf, auditory nerve fibre; IHC, inner hair cell; is, inner sulcus; Ko, Kölliker's organ (outlined in red); OHC, outer hair cell; tm, tectorial membrane (adapted from refs 9–11). **b**, **c**, Spontaneous activity recorded in voltage-clamp (**b**) and current-clamp (**c**, resting membrane potential (V_m) = –86 mV) from a P7 supporting cell. **d**, Spontaneous extracellular potentials recorded from Kölliker's organ showing the effects of PPADS (50 μM), suramin (150 μM) and octanol (1 mM). **e**, Histogram showing the effects of antagonists on frequency (black) and amplitude (grey) of spontaneous extracellular potentials. Asterisk, $P < 0.0005$ versus ACSF; double asterisk, $P < 0.05$ versus ACSF; dagger, $P < 0.02$ versus 0 Ca^{2+} ACSF. Data in **e** represent mean ± s.e.m. The number of experiments is indicated in parentheses.

ATP induces changes in cell shape

While imaging acutely isolated organs of Corti, periodic changes in light scattering were detected around groups of supporting cells within Kölliker's organ (Fig. 2a–c; Supplementary Video 1a–c). These spontaneous optical changes occurred randomly throughout Kölliker's organ at a frequency of 0.034 ± 0.003 Hz ($n = 15$), and were also observed along the thin processes of phalangeal cells, supporting cells that separate adjacent IHCs (Fig. 2d). In contrast, spontaneous optical changes were never observed near outer hair cells or in the outer sulcus. High-magnification imaging revealed that these local changes in transmittance resulted from an increase in extracellular space after crenation of inner supporting cells (Supplementary Fig. 4). As with the electrical activity recorded in this region, spontaneous optical changes were inhibited 94 ± 4% by PPADS ($n = 8$, $P < 0.0001$), 94 ± 2% by suramin ($n = 7$, $P < 0.0001$) and 91 ± 4% by octanol ($n = 7$, $P < 0.0001$; Fig. 2e), and could be elicited by focal application of ATP or UTP to Kölliker's organ (Supplementary Fig. 3). In experiments where imaging was performed simultaneously with whole-cell recording from inner supporting cells, 93% of spontaneous optical changes were found to be associated with spontaneous inward currents ($n = 380$ optical events in 12 cochleae; Fig. 2f), indicating that spontaneous optical changes result from the same endogenous ATP release events that mediate inward currents in supporting cells. Thus, intrinsic optical changes provide a non-invasive method for monitoring the spatial and temporal dynamics of ATP release in the organ of Corti.

Time-lapse imaging revealed that these optical changes propagated in a wave-like manner among supporting cells at 5 to 15 μm s^{-1} (Fig. 2a–c; Supplementary Video 1a–c), rates comparable to the propagation of ATP-dependent Ca^{2+} waves among astrocytes[21]. In cochlear explant cultures loaded with the Ca^{2+} indicator dye fura-2, we observed spontaneous elevations of intracellular Ca^{2+} within the supporting cells of Kölliker's organ that propagated as waves ($n = 7$ cochleae; Fig. 2g). Simultaneous differential interference contrast (DIC) and fluorescence imaging revealed that these Ca^{2+} transients either preceded or occurred coincident with spontaneous optical changes ($n = 23$; Fig. 2g, h), indicating that crenation follows the rise in intracellular Ca^{2+} concentration ($[Ca^{2+}]_i$). The frequency of spontaneous Ca^{2+} transients, like spontaneous optical changes, was decreased 80 ± 9% by suramin ($n = 4$, $P < 0.003$). These results suggest that extracellular ATP activates purinergic autoreceptors on inner supporting cells, leading to a rise in $[Ca^{2+}]_i$ and crenation. Supporting cells lateral to IHCs (for example, Deiters' cells, Hensen cells) also express purinergic receptors, and focal application of ATP to these cells triggered Ca^{2+} waves that propagated radially[22] (Supplementary Fig. 5). However, spontaneous Ca^{2+} waves were never observed in these cells ($n = 16$ cochleae). Together, these results suggest that ATP is primarily released from supporting cells within Kölliker's organ.

ATP excites hair cells and afferent nerve fibres

Previous studies have demonstrated that purinergic receptors are also expressed by IHCs and SGNs[23,24]. As most ATP-dependent spontaneous optical changes originated close to IHCs (Fig. 2d), we

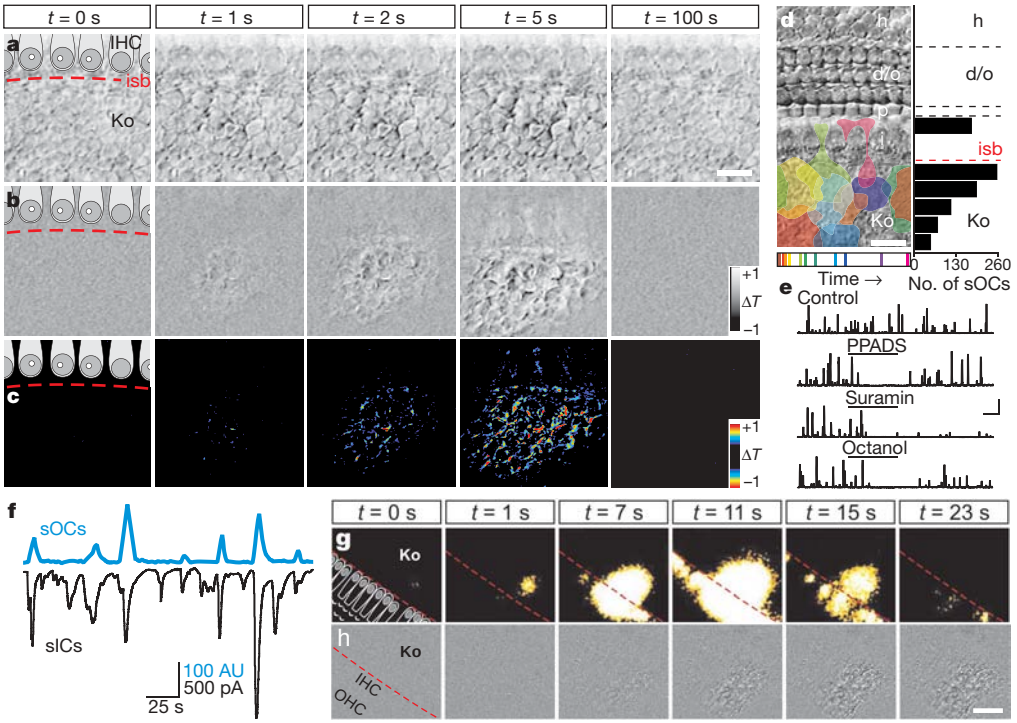

Figure 2 | ATP release elicits optical changes and intercellular Ca^{2+} waves in Kölliker's organ. **a**–**c**, Spontaneous optical changes within Kölliker's organ. **a**, Sequence of DIC images at indicated times (t). Dashed line demarcates the inner spiral bundle. **b**, Difference images after subtraction (see Methods). **c**, Pseudocoloured difference images after thresholding. **d**, Left: location and furthest extent of spontaneous optical changes (sOCs) during 300 s (time of occurrence is shown at the bottom). Right: distribution of origins of spontaneous optical changes in 10 μm bins ($n = 879$ events in 21 preparations). **e**, Plots of normalized transmittance changes (ΔT) over time; spontaneous optical changes are shown as upward deflections. Scale: 400 AU (arbitrary units), 200 s. **f**, Simultaneous recording of supporting cell spontaneous inward currents (black) and spontaneous optical changes (blue) from Kölliker's organ. sICs, spontaneous inward currents. **g**, **h**, Simultaneous time-lapse imaging of $[Ca^{2+}]_i$ (**g**) and intrinsic optical changes (difference images, **h**). d/o, Deiters' and outer hair cells; h, Hensen cells; i/IHC, inner hair cells; isb, inner spiral bundle; Ko, Kölliker's organ; OHC, outer hair cells; p, pillar cells. Scale bars for **a**–**c**, 15 μm; **d**, 20 μm, **g**, **h**, 30 μm.

investigated whether the periodic release of ATP also affected IHCs. When care was taken to maintain the integrity of the tissue, we detected spontaneous inward currents in all IHCs ($n = 35$), which occurred at a frequency of 0.053 ± 0.003 Hz (Fig. 3a) and ranged in amplitude from –8 to –180 pA (mean = –23.0 ± 0.9 pA, coefficient of variance = 0.71 ± 0.03; Fig. 3b). To determine the relationship between these slow currents ($t_{rise} = 2{,}222 \pm 80$ ms) and the activity recorded from inner supporting cells, we recorded simultaneously from IHCs and nearby supporting cells while imaging intrinsic optical changes within Kölliker's organ. As shown in Fig. 3c, spontaneous currents in IHCs were coincident with both spontaneous inward currents in supporting cells and spontaneous optical changes, suggesting that IHCs respond to the same ATP release events. Consistent with this hypothesis, PPADS and suramin decreased the frequency of spontaneous IHC currents by 92 ± 4% and 89 ± 4%, respectively ($n = 5$, $P < 0.0001$; Supplementary Fig. 6). The membrane conductance of IHCs increased by as much as 28% during these events, and the magnitude of the conductance change was proportional to the size of the current ($r = 0.82$, $n = 97$ events in four IHCs), consistent with the activation of ionotropic P2 receptors. Current-clamp recordings from IHCs revealed that these inward currents depolarized IHCs by as much as 28 mV and were capable of triggering bursts of Ca^{2+} action potentials ($n = 18$; Fig. 3d). In the presence of PPADS, the resting membrane potential of IHCs remained stable, except for small efferent-induced hyperpolarizations[13]. Together, these results suggest that the primary excitatory drive to IHCs at this age comes from ATP released by supporting cells in Kölliker's organ.

Previous studies indicate that Ca^{2+} spikes in neonatal IHCs induce bursts of excitatory postsynaptic currents (EPSCs) in afferent dendrites[3]. To address whether ATP-induced depolarization of IHCs triggers Ca^{2+}-dependent release of glutamate at IHC-afferent synapses, we made whole-cell recordings from the dendritic enlargements of afferent neurons at the base of IHCs and measured their

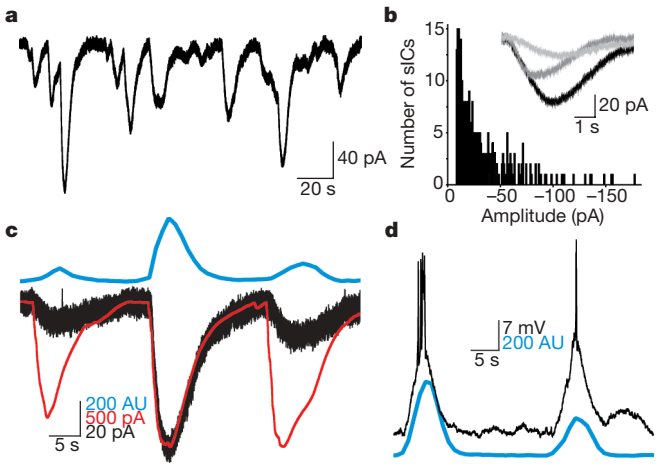

Figure 3 | Supporting-cell-derived ATP depolarizes IHCs. **a**, Spontaneous inward currents recorded from a P10 IHC. **b**, Amplitude distribution of spontaneous inward currents (sICs) recorded from IHC in **a**. Inset: three representative spontaneous inward currents. **c**, IHC spontaneous inward currents (black trace) were coincident with spontaneous inward currents recorded from a nearby inner supporting cell (red trace) and spontaneous optical changes (blue trace) imaged in the adjacent region of Kölliker's organ. **d**, Spontaneous depolarizations recorded from a P9 IHC (black trace; $V_m = -72$ mV) triggered Ca^{2+} spikes that were coincident with spontaneous optical changes (blue trace) in the adjacent region of Kölliker's organ.

response to exogenous ATP. In 7 out of 8 dendritic recordings, ATP application elicited a burst of EPSCs (Fig. 4a), presumably resulting from depolarization of and subsequent glutamate release from the presynaptic IHC. ATP also induced a slow inward current (–63 ± 18 pA, $n = 8$) that reversed near 0 mV, suggesting that ATP has a direct excitatory effect on these afferents. In current-clamp recordings, ATP triggered a burst of excitatory postsynaptic potentials in afferent dendrites ($n = 4$ of 5 recordings; Fig. 4b) that was blocked by NBQX ($n = 3$), indicating that the ATP-induced increase in activity requires glutamate release from IHCs.

To determine whether spontaneous release of ATP by inner supporting cells is sufficient to elicit transmitter release from IHCs, we monitored spontaneous optical changes in the region where

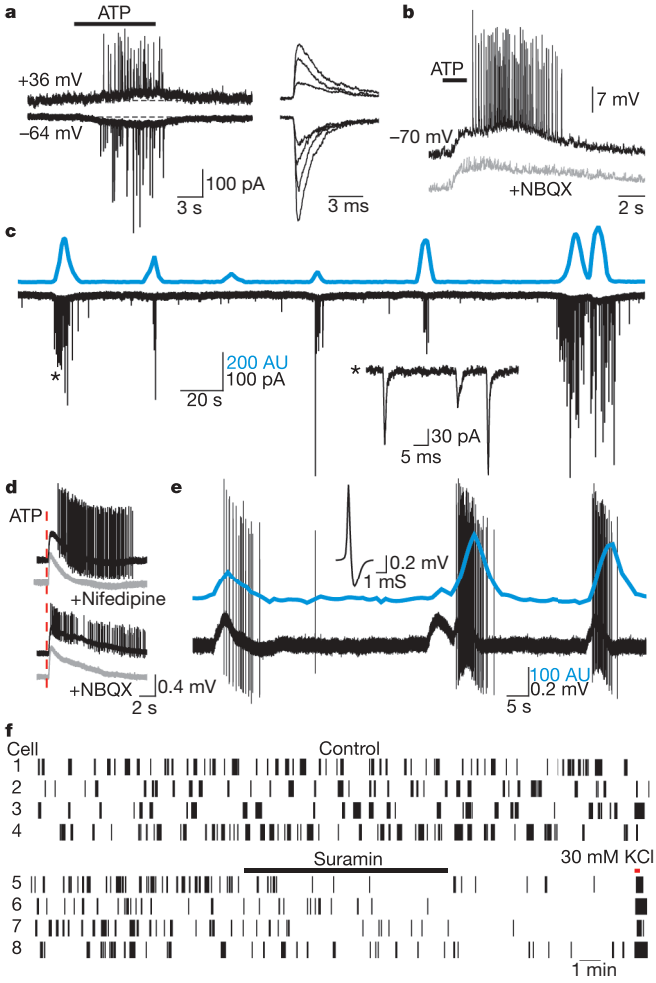

Figure 4 | Supporting-cell-derived ATP triggers bursts of action potentials in auditory nerve fibres. a, Voltage-clamp recording from an afferent dendrite showing a burst of EPSCs elicited by ATP. Right: EPSC detail. **b**, Current-clamp recording from an afferent dendrite showing block of ATP-induced excitatory postsynaptic potentials by NBQX. **c**, Simultaneous recording of spontaneous EPSCs from an afferent dendrite (black trace) and spontaneous optical changes (blue trace) imaged in the surrounding region. Inset: EPSC detail from region marked by asterisk. **d**, Loose-patch recordings from two SGNs showing activity in response to ATP-dependent stimulation of the presynaptic IHC in control (black traces) and in the presence of nifedipine or NBQX (grey traces). The slow positive deflection of the field (source wave) results from activation of ATP receptors in supporting cells. **e**, Simultaneous SGN loose-patch recording (black trace) and spontaneous optical changes (blue trace) imaged in the region around the presynaptic IHC. Inset, waveform of action potential. **f**, Raster plot of spontaneous action potentials from eight SGNs, in the absence (cells 1–4) or presence (cells 5–8) of suramin (100–250 μM). Application of ACSF containing 30 mM KCl confirmed IHC responsiveness.

dendritic recordings were made as an index of endogenous purinergic signalling. In four continuous recordings from afferent dendrites, discrete bursts of EPSCs occurred, separated by long periods with little synaptic activity (Fig. 4c). These bursts of EPSCs occurred at a frequency of 0.020 ± 0.005 Hz and lasted 6.9 ± 0.8 s ($n = 46$). Each burst was superimposed on a small increase in holding current (–7 ± 1 pA), similar to the responses elicited by exogenous ATP. Furthermore, 87% of EPSC bursts were coincident with spontaneous optical changes, and 71% of spontaneous optical changes originating within 50 μm of the terminals correlated with bursts, indicating that most ATP release events induce burst activity in nearby afferents.

To test whether extracellular ATP is responsible for initiating bursts of action potentials in auditory nerve fibres, we made loose-patch recordings from the somata of SGNs in cochlear whole mounts. When ATP was applied near the IHC presynaptic to the neuron being monitored, a train of action potentials was elicited ($n = 16$; Fig. 4d). This ATP-dependent increase in firing rate was blocked by nifedipine ($n = 3$) and NBQX ($n = 7$), indicating that it required Ca^{2+}-dependent glutamate release from IHCs. In continuous recordings from SGNs, discrete bursts of action potentials were observed at a frequency of 0.014 ± 0.001 Hz ($n = 11$; Fig. 4e), similar to the pattern of spontaneous EPSCs recorded from the dendrites of these neurons. Moreover, 90% of these bursts were coincident with spontaneous optical changes that occurred in the vicinity of the presynaptic IHC ($n = 244$ bursts). If this periodic firing is caused by spontaneous release of ATP, then it should be inhibited by purinergic receptor antagonists. Indeed, the frequency of spontaneous action potential bursts in SGNs was decreased 79 ± 8% by suramin ($n = 11$, $P = 0.0001$; Fig. 4f). These results indicate that bursts of action potentials in developing auditory nerve fibres are initiated by the periodic release of ATP from supporting cells in Kölliker's organ.

Spontaneous ATP signalling ceases at hearing onset

The pattern of auditory nerve fibre activity shifts from bursting to continuous discharge after the onset of hearing[25,26], suggesting that episodic activation of IHCs by ATP may decrease with age. To determine whether spontaneous purinergic signalling in the cochlea diminishes with development, we compared intrinsic ATP-mediated responses in organs of Corti isolated from rats before (P7–10) and after (P13–19) the onset of hearing[1,2]. We found that spontaneous optical changes, spontaneous extracellular potentials and spontaneous inward currents in IHCs were almost completely absent after the onset of hearing (Fig. 5). Thus, endogenous purinergic signalling in the cochlea follows the developmental change in the pattern of intrinsic activity observed *in vivo*. This rapid developmental down-regulation may help to ensure faithful representation of experience-dependent stimuli by minimizing spurious, sensory-independent activity in auditory pathways.

Hair cell activity is synchronized by ATP

Each ATP release event in Kölliker's organ is likely to affect multiple IHCs. We examined the relationship between the location and magnitude of these events and the amplitude of coincident spontaneous currents in IHCs (Fig. 6a, b). Spontaneous optical events that occurred near IHCs were associated with larger, faster rising currents (ratio of rise time to amplitude: 61 ± 3 ms pA^{-1}, $n = 175$ events in 8 cells) than events occurring further away (89 ± 6 ms pA^{-1}, $n = 78$, $P < 0.0001$). If IHCs exhibit similar sensitivity to ATP, neighbouring IHCs should experience similar activity. To determine whether the focal release of ATP is capable of synchronizing the output of neighbouring IHCs, we recorded spontaneous currents from pairs of IHCs located near (mean separation, $d = 68 \pm 6$ μm) or far ($d = 277 \pm 23$ μm) from one another. Whereas 91 ± 1% of spontaneous inward currents occurred synchronously in neighbouring hair cells ($n = 6$), only 22 ± 4% ($n = 6$, $P < 0.0001$) were correlated in IHCs separated by a distance corresponding to a frequency change

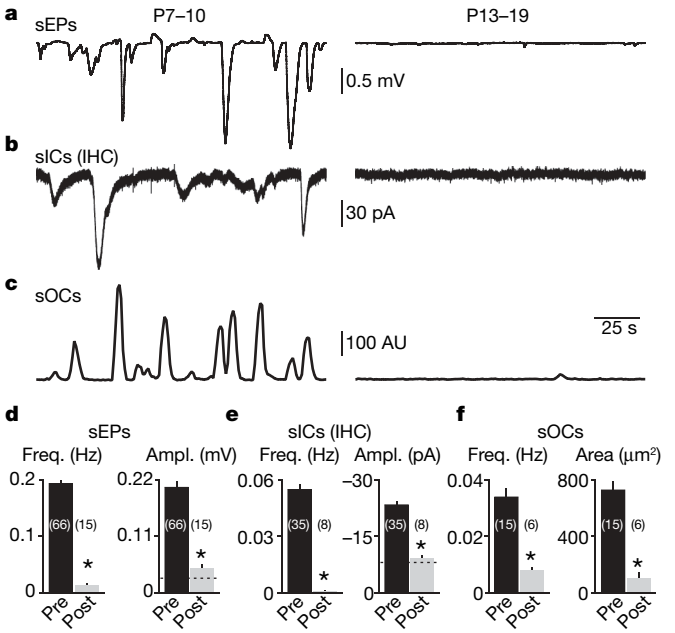

Figure 5 | Intrinsic purinergic signalling ceases after the onset of hearing. **a**–**c**, Spontaneous activity recorded from P7–10 (left) and P13–19 (right) cochleae. Spontaneous extracellular potentials (sEPs, **a**) and spontaneous optical changes (sOCs, **c**) were recorded in Kölliker's organ (left) or the inner sulcus (right). sICs, spontaneous inward currents. **d**–**f**, Plots of the frequency and amplitude of spontaneous extracellular potentials (**d**), spontaneous inward currents in IHCs (**e**) and spontaneous optical changes (**f**) before (age P7–10, pre) and after (age P13–19, post) hearing onset. The dashed lines indicate detection thresholds. Asterisk, $P < 0.0001$. Data in **d**–**f** represent mean ± s.e.m. The number of experiments is indicated in parentheses.

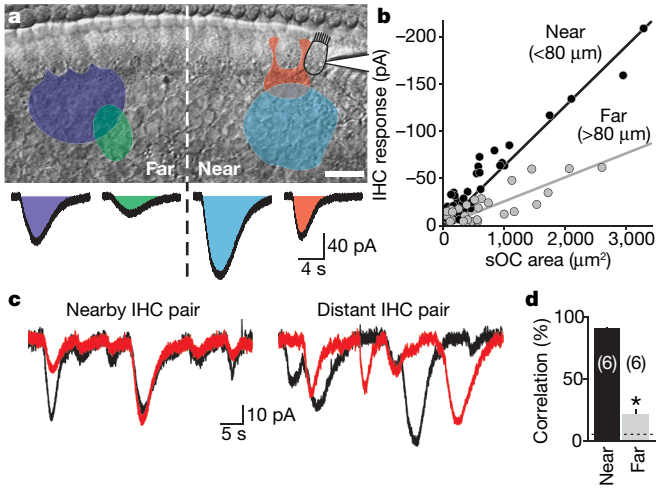

Figure 6 | Local release of ATP synchronizes the activity of neighbouring IHCs. **a**, Top: location and furthest extent of four spontaneous optical changes (pseudocolour overlay) recorded from one P9 organ of Corti. Bottom: coincident spontaneous inward currents recorded from one IHC (highlighted in top image). Scale: 20 μm. **b**, Plot of peak amplitude of spontaneous inward currents from the IHC shown in **a**, versus maximum area of coincident spontaneous optical changes. Responses are grouped according to location relative to the IHC. Lines are regression fits. **c**, Spontaneous inward currents recorded simultaneously from two IHCs located near (left) or far from (right) one another. **d**, Plot showing percentage correlation of spontaneous inward currents recorded from IHCs located near (black) or far (grey) from one another. The dashed line indicates correlation predicted by chance alone. Asterisk, $P < 0.0001$. Data in **d** represent mean ± s.e.m. The number of experiments is indicated in parentheses.

of one octave (~250 μm)[27] (Fig. 6c, d). These results indicate that purinergic signalling in the developing organ of Corti is capable of synchronizing transmitter release from IHCs that will encode similar frequencies. If Ca^{2+} spikes are required to trigger glutamate release from these immature IHCs[28,29], the number of auditory nerve fibres activated by each ATP-release event would be further restricted.

Discussion

Spontaneous activity in auditory nerve fibres before the onset of hearing is essential for the survival of target neurons in the cochlear nucleus, accurate wiring of auditory pathways, and the refinement of tonotopic maps in auditory nuclei[30–35]. Our findings indicate that supporting cells within Kölliker's organ initiate bursts of electrical activity in SGNs before the onset of hearing through ATP-dependent excitation of hair cells. These results suggest that peripheral, non-sensory cells are essential for the maturation of auditory pathways in the brain. This activity may combine with intrinsically generated Ca^{2+} spikes[29,36,37] to produce distinct patterns of activity before the onset of hearing.

Synchronous activity among groups of hair cells along the length of the cochlea could help establish and maintain tonotopic segregation of neuronal projections in auditory pathways through hebbian-like plasticity[31,38,39]. Although correlated activity of neighbouring IHCs would be expected to reinforce connections to discrete targets in the central nervous system, by itself this activity would not provide information about the tonotopic position of active hair cells along the cochlea. It is likely that genetically encoded guidance cues are responsible for initial targeting and segregation of inputs in auditory nuclei, as has been described in the visual system[40], whereas the periodic activity described here could help further refine and maintain synaptic connections[34,41].

Although spontaneous release of ATP ceases after hearing onset, hair cells and supporting cells in the mature cochlea continue to express P2 receptors[24,42], and cochlear injury triggers the release of ATP and induces Ca^{2+} waves in supporting cells[43]. If spontaneous release of ATP were re-established under these conditions, sensory-independent activity may re-emerge in the auditory nerve, leading to conditions such as peripheral tinnitus. In addition, ATP is a known trophic factor, mitogen and potent neuromodulator[44,45], raising the possibility that cells within Kölliker's organ participate in other vital aspects of cochlear development. A greater understanding of the mechanisms that regulate ATP release from cochlear supporting cells may help reveal new roles for this activity in the development and dysfunction of the auditory system.

METHODS SUMMARY

Apical cochlear coils were removed from postnatal day (P) 7 to P19 Sprague–Dawley rats and used within 3 h of the dissection. Whole-cell, voltage- and current-clamp recordings from inner supporting cells, IHCs and auditory nerve afferents were performed under visual control, as described previously[3,46]. Spontaneous optical changes were imaged with DIC optics using a charge-coupled device (CCD) camera, and acquired at a rate of 1 frame s^{-1}. Transmittance changes were visualized by subtracting images 5 s apart, and quantified by applying a thresholding function to highlight changing pixels. Frequency measurements of spontaneous optical changes were normalized for a 10^4 μm^2 imaging area. Extracellular recordings of action potentials from SGNs and Ca^{2+} imaging were performed in cochlear organotypic cultures maintained for 1 to 7 days *in vitro*. Spontaneous and evoked changes in intracellular Ca^{2+} were monitored in cultures loaded with fura-2 or fluo-4 AM dyes, as described[43]. Statistical comparisons were made using paired or independent, two-tailed Student's *t*-tests assuming unequal variance, and significance was concluded when $P < 0.05$. Data are reported as mean ± standard error of the mean (s.e.m.). Experiments were carried out in artificial cerebrospinal fluid (ACSF) at ambient temperature.

Full Methods and any associated references are available in the online version of the paper at www.nature.com/nature.

Received 1 June; accepted 10 September 2007.

1. Geal-Dor, M., Freeman, S., Li, G. & Sohmer, H. Development of hearing in neonatal rats: air and bone conducted ABR thresholds. *Hear. Res.* **69**, 236–242 (1993).

2. Puel, J. L. & Uziel, A. Correlative development of cochlear action potential sensitivity, latency, and frequency selectivity. *Brain Res.* **465,** 179–188 (1987).
3. Glowatzki, E. & Fuchs, P. A. Transmitter release at the hair cell ribbon synapse. *Nature Neurosci.* **5,** 147–154 (2002).
4. Gummer, A. W. & Mark, R. F. Patterned neural activity in brain stem auditory areas of a prehearing mammal, the tammar wallaby (*Macropus eugenii*). *Neuroreport* **5,** 685–688 (1994).
5. Jones, T. A., Jones, S. M. & Paggett, K. C. Primordial rhythmic bursting in embryonic cochlear ganglion cells. *J. Neurosci.* **21,** 8129–8135 (2001).
6. Jones, T. A., Leake, P. A., Snyder, R. L., Stakhovskaya, O. & Bonham, B. H. Spontaneous discharge patterns in cochlear spiral ganglion cells prior to the onset of hearing in cats. *J. Neurophysiol.* doi:10.1152/jn.00472.2007 (8 August 2007).
7. Walsh, E. J. & McGee, J. Postnatal development of auditory nerve and cochlear nucleus neuronal responses in kittens. *Hear. Res.* **28,** 97–116 (1987).
8. Lippe, W. R. Rhythmic spontaneous activity in the developing avian auditory system. *J. Neurosci.* **14,** 1486–1495 (1994).
9. Retzius, G. *Das Gehörorgan der Wirbelthiere*. II. *Das Gehörorgan der Reptilien, der Vögel und Säugethiere* (Samson & Wallin, Stockholm, 1884).
10. Hinojosa, R. A note on development of Corti's organ. *Acta Otolaryngol. (Stockh.)* **84,** 238–251 (1977).
11. Wada, T. Anatomical and physiological studies on the growth of the inner ear of the albino rat. *Am. Anat. Mem.* **10,** 1–174 (1923).
12. Eybalin, M. Neurotransmitters and neuromodulators of the mammalian cochlea. *Physiol. Rev.* **73,** 309–373 (1993).
13. Glowatzki, E. & Fuchs, P. A. Cholinergic synaptic inhibition of inner hair cells in the neonatal mammalian cochlea. *Science* **288,** 2366–2368 (2000).
14. Fuchs, P. A., Evans, M. G. & Murrow, B. W. Calcium currents in hair cells isolated from the cochlea of the chick. *J. Physiol. (Lond.)* **429,** 553–568 (1990).
15. Burnstock, G. Physiology and pathophysiology of purinergic neurotransmission. *Physiol. Rev.* **87,** 659–797 (2007).
16. Housley, G. D. Physiological effects of extracellular nucleotides in the inner ear. *Clin. Exp. Pharmacol. Physiol.* **27,** 575–580 (2000).
17. North, R. A. Molecular physiology of P2X receptors. *Physiol. Rev.* **82,** 1013–1067 (2002).
18. Bennett, M. V., Contreras, J. E., Bukauskas, F. F. & Saez, J. C. New roles for astrocytes: gap junction hemichannels have something to communicate. *Trends Neurosci.* **26,** 610–617 (2003).
19. Forge, A. *et al.* Gap junctions in the inner ear: comparison of distribution patterns in different vertebrates and assessment of connexin composition in mammals. *J. Comp. Neurol.* **467,** 207–231 (2003).
20. Zhao, H. B. Connexin26 is responsible for anionic molecule permeability in the cochlea for intercellular signalling and metabolic communications. *Eur. J. Neurosci.* **21,** 1859–1868 (2005).
21. Charles, A. & Giaume, C. *Intercellular Calcium Waves in Astrocytes: Underlying Mechanisms and Functional Significance* (eds Volterra, A., Magistretti, P. J. & Haydon, P. G.) (Oxford Univ. Press, Oxford, 2002).
22. Piazza, V., Ciubotaru, C. D., Gale, J. E. & Mammano, F. Purinergic signalling and intercellular Ca^{2+} wave propagation in the organ of Corti. *Cell Calcium* **41,** 77–86 (2007).
23. Salih, S. G., Jagger, D. J. & Housley, G. D. ATP-gated currents in rat primary auditory neurones *in situ* arise from a heteromultimetric P2X receptor subunit assembly. *Neuropharmacology* **42,** 386–395 (2002).
24. Sugasawa, M., Erostegui, C., Blanchet, C. & Dulon, D. ATP activates non-selective cation channels and calcium release in inner hair cells of the guinea-pig cochlea. *J. Physiol. (Lond.)* **491,** 707–718 (1996).
25. Jones, T. A. & Jones, S. M. Spontaneous activity in the statoacoustic ganglion of the chicken embryo. *J. Neurophysiol.* **83,** 1452–1468 (2000).
26. Rübsamen, R. & Lippe, W. R. in *Development of the Auditory System* (eds Rubel, E. W., Popper, A. N. & Fay, R. R.) 193–270 (Springer, New York, 1998).
27. Müller, M. Frequency representation in the rat cochlea. *Hear. Res.* **51,** 247–254 (1991).
28. Beutner, D. & Moser, T. The presynaptic function of mouse cochlear inner hair cells during development of hearing. *J. Neurosci.* **21,** 4593–4599 (2001).
29. Marcotti, W., Johnson, S. L., Rüsch, A. & Kros, C. J. Sodium and calcium currents shape action potentials in immature mouse inner hair cells. *J. Physiol. (Lond.)* **552,** 743–761 (2003).
30. Friauf, E. & Lohmann, C. Development of auditory brainstem circuitry. Activity-dependent and activity-independent processes. *Cell Tissue Res.* **297,** 187–195 (1999).
31. Kandler, K. Activity-dependent organization of inhibitory circuits: lessons from the auditory system. *Curr. Opin. Neurobiol.* **14,** 96–104 (2004).
32. Rubel, E. W. & Fritzsch, B. Auditory system development: primary auditory neurons and their targets. *Annu. Rev. Neurosci.* **25,** 51–101 (2002).
33. Leao, R. N. *et al.* Topographic organization in the auditory brainstem of juvenile mice is disrupted in congenital deafness. *J. Physiol. (Lond.)* **571,** 563–578 (2006).
34. Leake, P. A., Hradek, G. T., Chair, L. & Snyder, R. L. Neonatal deafness results in degraded topographic specificity of auditory nerve projections to the cochlear nucleus in cats. *J. Comp. Neurol.* **497,** 13–31 (2006).
35. Gabriele, M. L., Brunso-Bechtold, J. K. & Henkel, C. K. Plasticity in the development of afferent patterns in the inferior colliculus of the rat after unilateral cochlear ablation. *J. Neurosci.* **20,** 6939–6949 (2000).
36. Kros, C. J., Rüppersberg, J. P. & Rüsch, A. Expression of a potassium current in inner hair cells during development of hearing in mice. *Nature* **394,** 281–284 (1998).
37. Marcotti, W., Johnson, S. L., Holley, M. C. & Kros, C. J. Developmental changes in the expression of potassium currents of embryonic, neonatal and mature mouse inner hair cells. *J. Physiol. (Lond.)* **548,** 383–400 (2003).
38. Katz, L. C. & Shatz, C. J. Synaptic activity and the construction of cortical circuits. *Science* **274,** 1133–1138 (1996).
39. Kotak, V. C. & Sanes, D. H. Synaptically evoked prolonged depolarizations in the developing auditory system. *J. Neurophysiol.* **74,** 1611–1620 (1995).
40. Huberman, A. D. Mechanisms of eye-specific visual circuit development. *Curr. Opin. Neurobiol.* **17,** 73–80 (2007).
41. Erazo-Fischer, E., Striessnig, J. & Taschenberger, H. The role of physiological afferent nerve activity during *in vivo* maturation of the calyx of Held synapse. *J. Neurosci.* **27,** 1725–1737 (2007).
42. Lagostena, L. & Mammano, F. Intracellular calcium dynamics and membrane conductance changes evoked by Deiters' cell purinoceptor activation in the organ of Corti. *Cell Calcium* **29,** 191–198 (2001).
43. Gale, J. E., Piazza, V., Ciubotaru, C. D. & Mammano, F. A mechanism for sensing noise damage in the inner ear. *Curr. Biol.* **14,** 526–529 (2004).
44. Fields, R. D. & Burnstock, G. Purinergic signalling in neuron–glia interactions. *Nature Rev. Neurosci.* **7,** 423–436 (2006).
45. Nedergaard, M., Ransom, B. & Goldman, S. A. New roles for astrocytes: redefining the functional architecture of the brain. *Trends Neurosci.* **26,** 523–530 (2003).
46. Glowatzki, E. *et al.* The glutamate-aspartate transporter GLAST mediates glutamate uptake at inner hair cell afferent synapses in the mammalian cochlea. *J. Neurosci.* **26,** 7659–7664 (2006).

Supplementary Information is linked to the online version of the paper at www.nature.com/nature.

Acknowledgements We thank J.-H. Kong for help with preliminary experiments, and P. Fuchs, J. Howell and M. Lahne for discussions. This work was supported by a Royal Society University Research Fellowship (to J.E.G.), National Institutes of Health Grants (to E.G. and D.E.B.) and the Deafness Research Foundation (to D.E.B.).

Author Information Reprints and permissions information is available at www.nature.com/reprints. Correspondence and requests for materials should be addressed to dbergles@jhmi.edu.

METHODS

Tissue preparation. All experimental protocols were approved by the Johns Hopkins University Animal Care and Use Committee. Apical turns of postnatal day (P) 7 to 19 (day of birth is P0) Sprague–Dawley rat cochleae were isolated in ice-cold artificial cerebral spinal fluid (ACSF) containing (in mM): NaCl (119), KCl (2.5), $CaCl_2$ (2.5), $MgCl_2$ (1.3), NaH_2PO_4 (1), $NaHCO_3$ (26.2) and glucose (11), saturated with 95% O_2/5% CO_2. Other than the stria vascularis and tectorial membrane, which were gently peeled off, the cellular organization of the organ of Corti was left intact. Acutely isolated cochlear turns were transferred to a Plexiglas chamber mounted on an upright microscope (Zeiss Axioskop FS2) and imaged using infrared light (~770 nm) and DIC optics using a charge-coupled device (CCD) camera (Sony XC-73). Organs of Corti were continually superfused with ACSF at 22–24 °C, and used within 3 h of the dissection. For afferent dendrite recordings, the bath solution contained (in mM): NaCl (144), KCl (5.8), $CaCl_2$ (1.3), $MgCl_2$ (0.9), NaH_2PO_4 (0.7), HEPES (10) and glucose (5.6), pH 7.4. For organotypic cultures, P1–7 cochlear turns were plated on Cell-Tak-coated (BD Biosciences) coverslips and maintained for 1 to 7 days *in vitro* in F12/DMEM (Invitrogen) supplemented with 1% fetal bovine serum. Ca^{2+} imaging was performed as described previously[43].

Electrophysiology. Whole-cell, voltage- and current-clamp recordings from supporting cells, IHCs and auditory nerve dendrites were performed under visual control as described previously[3,46]. Electrodes were advanced through the tissue under minimal positive pressure to limit cellular disruption. Intracellular solutions were composed of the following (in mM): KCH_3SO_3 (134), HEPES (20), EGTA (10), $MgCl_2$ (1), pH 7.3. For IHC recordings, the electrode solution was supplemented with Na_2ATP (2 mM) and NaGTP (0.2 mM) to allow long and stable recordings. In the presence of 2.5 mM KCl, IHCs in P7–10 organs of Corti had a resting membrane potential (V_m) of approximately −75 mV and did not fire tonically. For afferent recordings, the internal solution contained (in mM): KCl (150), $MgCl_2$ (3.5), $CaCl_2$ (0.1), EGTA (5), HEPES (5), pH 7.2. Nucleotides were omitted from most internal solutions to minimize P2 receptor desensitization (see Supplementary Fig. 3). Extracellular action potentials were recorded from SGNs by making low-resistance seals (~15 MΩ) with their somata. Pipette resistances were 1–2 MΩ for field- and loose-patch recordings, 2–4 MΩ for whole-cell recordings, and 10−15 MΩ for afferent dendrite recordings. During voltage-clamp recordings, the membrane potentials of IHCs, afferent dendrites, and supporting cells were held at −80 mV, −84 mV and −90 mV, respectively, unless otherwise indicated. Errors due to the voltage drop across the series resistance were left uncompensated. Membrane voltage and currents were recorded with pClamp9 software using a Multiclamp 700A amplifier, low-pass filtered at 0.1–10 kHz, and digitized at 10–50 kHz with a Digidata 1322A analogue to digital converter (Molecular Devices). Data were analysed off-line using Clampfit (Molecular Devices) and Origin (Microcal Software) software. Spontaneous extracellular potentials and supporting cell spontaneous inward currents with amplitudes above baseline noise (0.03 mV and 8 pA, respectively) were measured and deemed correlated when they occurred within ±250 ms. The mean field potential amplitude was calculated from absolute values. IHC currents were considered coincident when their peaks occurred within ±500 ms of one another. EPSC and action potential bursts were defined as groups of a minimum of four events occurring at a frequency greater than 2.4 Hz (mean frequency: 8.14 ± 1.11 Hz, $n = 46$) that differed significantly from the mean EPSC frequency between bursts (0.17 ± 0.03 Hz, $P < 0.0001$). For pharmacological studies, a stable baseline was recorded for 20 min, then one of the following drugs (all from Sigma, unless specified otherwise) was superfused for 10 min: PPADS (50 μM; Tocris), suramin (100–250 μM, unless indicated otherwise; Tocris), octanol (1 mM), carbenoxolone (500 μM), strychnine (1 μM); D-tubocurarine (10 μM), atropine (3 μM), TTX (1 μM; Alamone), nifedipine (50 μM; Tocris), NBQX (10 μM; Tocris), *R*,*S*-CPP (10 μM; Tocris), DPCPX (5 μM; Tocris), TNP-ATP (1 μM; Tocris), brilliant blue G (10 μM), $CdCl_2$ (30 μM), followed by a 20 to 30 min recovery period. Apyrase (50 U ml^{-1}; Sigma) was applied for 30 min under static bath in HEPES-buffered ACSF, pH 7.4. In each case, the mean absolute amplitude and frequency were calculated for 200-s bins, normalized to baseline averages, and for statistical analysis compared to values obtained at corresponding times in control preparations continuously bathed in ACSF. Only one drug was applied per cochlear turn. For focal application of nucleotides, the agonists were dissolved in HEPES-buffered ACSF to a concentration of 100 μM, loaded into a patch pipette, and expelled from the tip using a Picospritzer (50–100 ms, 5 p.s.i.). Statistical comparison of means was made using paired or independent, two-tailed Student's *t*-tests assuming unequal variance, and significance was concluded when $P < 0.05$. Data are presented as mean ± s.e.m.

Intrinsic optical imaging. Cochlear turns were imaged with a ×40 water immersion objective coupled to an additional ×0.5–2.0 adjustable zoom lens (Zeiss) to allow low-magnification imaging of 220-μm-long cochlear segments after whole-cell recordings were established at high-magnification. IR-DIC images were acquired at 1 frame per second using an LG-3 frame grabber card (Scion Corporation) and Scion Image software. Difference movies were created by subtracting frames captured at times t_n and t_{n+5} seconds from each other using ImageJ software, to provide an index of transmittance change (ΔT) over time: stable regions are depicted in grey, whereas regions undergoing spontaneous optical changes appear black and white. To quantify intrinsic optical changes, a thresholding function was applied to highlight and count pixels that changed (in arbitrary units, AU). Identical contrast and threshold values were used to quantify all movies in a given experiment. Spontaneous optical change frequency measurements were normalized for a 10^4 μm^2 imaging area. Plots of transmittance change over time were precisely aligned to electrophysiological traces by taking into consideration the 5-s lag artificially created through the image subtraction process.